OLLSCOIL NA GAILLIMHE
UNIVERSITY OF GALWAY

Biochemistry Research Project BI453

Academic Year 2024/25

In Vivo Analysis of the Epigenetic Landscape in Hydractinia symbiolongicarpus

Examination candidate's name: Rowan Allan

ID number: 21470276

Academic supervisor: Uri Frank

Course: Genetics/ Genomics

OLLSCOIL NA GAILLIMHE
UNIVERSITY OF GALWAY

BI453 Research Report

Plagiarism Declaration

This form must be signed by the student, and must be included in the final submitted research report.

Student name: Rowan Allan

ID number: 21470276

Report title: *In Vivo* Analysis of the Epigenetic Landscape in Hydractinia symbiolongicarpus

Supervisor: Uri Frank

I hereby certify that this report is entirely my own work, and that the contents of this essay have not been published elsewhere in either paper or electronic form unless indicated otherwise through referencing.

Rowan Allan _____ 28/03/25

Signature Date

The University of Galway official Student Code of Conduct is at
https://www.universityofgalway.ie/media/studentservices/files/QA-616-University-of-Galway-Student-Code-of-Conduct-(Oct-2022).pdf
and the Academic Integrity Policy is at
https://www.universityofgalway.ie/media/registrar/docs/policiesmay2023/QA220-Academic-Integrity-Policy-v2.0-Sept-2023.pdf

Table of Contents

Acknowledgements

Thank you to Prof Uri Frank for the continued support throughout this project. You were a brilliant supervisor, and I am so grateful for the opportunity I had to be a part of your lab. I am thankful for your guidance and feedback, you always had time to answer my questions no matter how busy you were.

I would also like to thank PhD student Paris Weavers. You were such a great companion throughout this project. You always had an answer for every single one of my questions . Thank you for all your advice and mentoring, I really appreciate it.

1. Lay Abstract

Although all cells in an organism share an identical genome, they exhibit a diverse range of functions due to differential gene expression. This is often controlled by epigenetics, which comes from “epi” meaning “on top of”. It involves chemical alterations to DNA and histones without changing the underlying DNA sequence itself. Most research on epigenetics comes from *in vitro* culture systems, but we studied them in a living marine animal called *Hydractinia symbiolongicarpus*. We found that a key epigenetic regulator called *DNMT3* exhibits a high level of activity in the stem cell population of this organism. We also identified differences in how DNA is packaged in different cell types by staining histone modifications. These findings can help us understand how cells maintain their identity, which has implications for stem cell research and regenerative medicine.

2. Scientific Abstract

Major epigenetic modifications like DNA methylation and histone modifications, play an essential role in inducing and maintaining cell identity through regulation of gene expression. However, much of our understanding of these processes comes from *in vitro* studies. This study investigates the epigenetic landscape of the cnidarian *Hydractinia symbiolongicarpus in vivo* allowing for comparison across different cell types, providing a unique opportunity to study epigenetic regulation. Using comparative genomics and single-cell transcriptomics, we identified a DNMT3a homolog enriched in pluripotent interstitial cells (i-cells) and progenitor cell populations, suggesting a role in de novo DNA methylation and epigenetic plasticity. We employed signal amplification by exchange reaction (SABER) - fluorescent in situ hybridisation (FISH) to determine DNMT3 expression *in vivo* and further validate its expression in i-cells. Immunofluorescence analysis of H3K9me3 and H4K16ac *in vivo* revealed distinct chromatin organisation across different cell types. This study provides a comprehensive framework for further functional studies of key epigenetic regulators and the regulatory networks that define cell types in *Hydractinia*.

3. List of Abbreviations

i-cells	Interstitial cells
SABER	Saber amplification by exchange reaction
FISH	Fluorescent in situ hybridisation
DNMT	DNA methyltransferase
TSS	Transcription start sites
CDD	Conserved Domain Database
HP1	Heterochromatin protein 1
DAPI	4’,6-diamidino-2-phenylindole
ROI	Region of interest
CV	Coefficient of variation
PCC	Pearson’s correlation coefficient
M1	Mander’s coefficient
ADD	ATRX-DNMT3-DNMT3L
DCM	DNA methyltransferase catalytic motif
JaCoP	Just Another Colocalization Plugin

4. Introduction

Most eukaryotic chromosomes despite their great variety and complexity in different organisms, share fundamental principles of organisation. The chromosomal material also known as chromatin, contains DNA and proteins called histones [1]. Eight histones, two each of H2A, H2B, H3 and H4 form the histone core octamer while the H1 linker histone binds outside the complex [2]. Histones are complexed with DNA in a repeating pattern called the nucleosome. Nucleosomes exists in different states of compaction which regulate the accessibility to the transcriptional machinery, thereby influencing cellular identity [1]. The majority of chromatin exists as heterochromatin in pericentric regions, telomeres, and other repressed genomic areas. Heterochromatin is formed of tightly condensed nucleosome that is transcriptionally inactive. In contrast, euchromatin is more open and loosely packed [3].

Key modifications can be made to nucleotide residues or histones encompassed in the nucleosome, termed epigenetic modifications. Epigenetic comes from "epi" meaning "on top of", influencing gene expression without altering the DNA sequence. DNA methylation and histone modifications are two major classes of epigenetic modifiers that play major roles in cell function and identity [4].

DNA methylation involves the addition of a methyl group to the 5-position of cytosine, predominantly within CpG islands which are disproportionably located in promoter regions. A family of DNA methyltransferases (DNMTs) including DNMT3 and DNMT1 are responsible for methylation [5]. DNMT1 primarily maintains methylation patterns across cell cyles while DNMT3 is a de novo methyltransferase, responsible for establishing new patterns [5]. When promoters and transcription sites are methylated, activating transcription factors can be blocked and/or chromatin remodelling complexes that enforce a repressive state are recruited [5].

Histone modifications occur post-translationally on the tail domains of histones. Hundreds of histone modifications altering cell activity have been identified. These include ubiquitination, acetylation and methylation states of lysine residues, particularly in histones 3 and 4 [2]. While three methyl groups can be deposited on the lysine residues, acetylation only occurs singly. The genomic location of these individual modifications and their combinatorial patterns are known as the "histone code" [6]. Histone modifications influence nucleosome spacing, affecting chromatin compaction. They can facilitate the recruitment of histone-modifying complexes that activate or repress gene expression similarly to DNA methylation [7].

The post-translational trimethylation of histone H3 at lysine 9 (H3K9me3) is an established marker of constitutive and facultative heterochromatin [6]. It is catalysed by the lysine methyltransferase and erased by lysine demethylase [6]. Histone methylation can directly influence chromosome structure. However, its functional outcomes are primarily determined by reader proteins, which recognise methylated histones and recruit additional factors to regulate chromatin dynamics [8]. A small conserved chromosomal protein known as heterochromatin protein 1 (HP1) is a well-studied effector. The variant HP1a induces heterochromatin formation via nucleosome cross-linking and recruitment of additional factors [9].

In contrast to the repressive role of H3K9me3, histone H4 acetylation at lysine 16 is a hallmark of open chromatin [10]. This modification neutralises the positive charge of lysine 16, thereby reducing the electrostatic interactions between histone tails and DNA. It is catalysed by the histone acetyltransferase MOF which is tightly regulated by various signalling pathways and interacting proteins [10]. H4K16ac may be the founding acetylation event on H4, serving as a key regulatory mechanism that influences subsequent histone acetylation patterns [10].

Much of our understanding of chromatin organisation and epigenetic regulation comes from studies in vertebrate models such as mice and human cell cultures. However, multiple cnidarians have emerged as valuable models for studying chromatin because of their unique biological traits, including their continuous cell proliferation and presence of adult stem cells [2]. The fragmentary nature of the literature on cnidarian epigenetics and histones suggests there is significant potential for uncovering novel insights into chromatin dynamics and cellular regulation [2].

One such model cnidarian is *Hydractinia symbiolongicarpus. Hydractinia* is a marine colonial hydroid and it was the first organism in which germline precursors were explicitly referred to as “stem cells” [11]. *Hydractinia* is amenable to genetic manipulation, and there are established methods for visualising proteins using immunofluorescence and RNA expression *in situ,* respectively [12]. This allows for comparison across cell types, providing a unique opportunity to study epigenetic regulation.

The main characterised stem cells in *Hydractinia* are called interstitial cells (i-cells) and they retain pluripotency throughout their lifespan. The high expression of *Piwi1* and *Piwi2* serve as key markers of i-cells. i-cells have the capacity to differentiate into all cell types of the animal throughout adulthood, like epithelial and nematocyte cells (Fig. 1A) [13]. They can also commit to neuronal lineages, where their final stage of differentiation is marked by expression of markers such as Elav1 and RFamide [12]. The transcriptional profile of these cell types reflects their distinct functional roles. i-cells exhibit high chromatin accessibility at transcription start sites (TSS), consistent with their pluripotent nature and active transcriptional state. In contrast, neurons and nematocytes display a more restricted accessibility pattern, suggesting lineage-specific transcriptional regulation (Fig. 1B). Given that chromatin organisation and histone modifications are key determinants of gene expression, these factors likely play a crucial role in governing the transcriptional profiles of different cell types

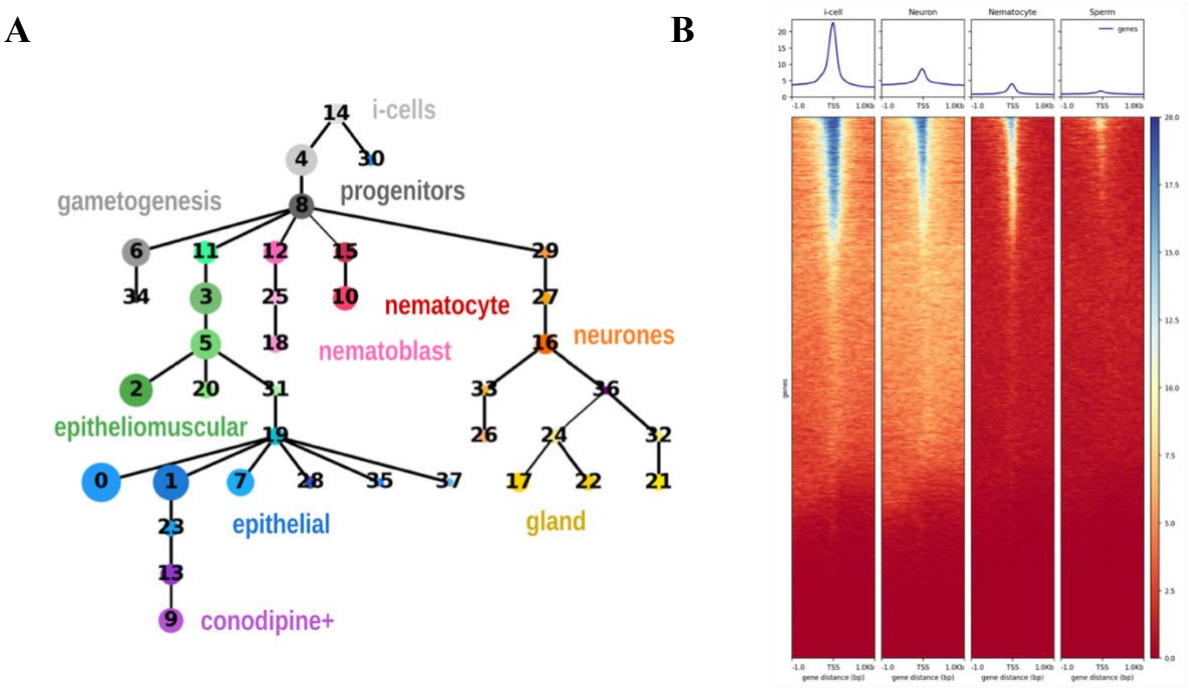

Figure 1. Partition-based graph abstraction of *Hydractinia* single-cell transcriptomes. ***(A)*** *Each node represents a transcriptionally distinct cluster based on RNA expression data, with node size proportional to the number of cells within the cluster. Edges correspond to the connectivity between clusters, indicating likely differentiation trajectories. Adapted from [14].* ***(B)*** *Heatmap showing the average gene expression patterns across different cell types in relation to genomic distance from TSS. Mac Gabhann, unpublished data.*

Despite some characterisation of histones in *Hydractinia*, very little has been done to explore the role of key epigenetic modifiers like DNA methylation, histone methylation and histone acetylation [2]. This study aims to identify and characterise these factors involved in chromatin remodelling, following two different approaches. Firstly, we employ signal amplification by exchange reaction (SABER) - fluorescent in situ hybridisation (FISH) to determine DNMT3 expression *in vivo* and validate its expression in i-cells, which was previously suggested by single-cell RNA sequencing data [14]. Secondly, we perform immunofluorescence staining of H3K9me3 and H4K16ac to further characterise the epigenetic landscape of i-cells, while conducting quantitative and spacial comparisons of fluorescent antibody intensity against specific differentiated somatic cell types. This will therefore help to provide insights into the differing chromatin landscapes in stem cells and somatic tissue *in vivo* in a cnidarian.

5. Materials and Methods

5.1. Hydractinia Culture

Hydractinia symbiolongicarpus wild type 291-10 and the RFamide::GFP transgenic animal were cultured as previously described [15]. Feeding polyps were cut and collected using a fine surgical scissors close to the polyp-stolon boundary.

5.2. DNMT3a identification and RNA expression mapping

To identify potential DNMT homologs in *Hydractinia*, we retrieved protein sequences annotated in *Hydra*, a closely related hydrozoan cnidarian. A standard protein BLAST search was performed against the *Hydractinia* proteome and a candidate sequence was chosen based on high similarity. To further validate its functional relevance, we analysed the sequence using NCBI's Conserved Domain Database (CDD) to confirm the presence of domains associated with catalytic activity. The gene identifier was inputted into a computational pipeline allowing for its visualisation across different cell types using a single-cell atlas which was recently developed for *Hydractinia* [14].

5.3. SABER-FISH

SABER-FISH was carried out as previously outlined [14]. OligoMiner was used to design a set of high-specificity, thermodynamically stable probes for synthesis. The transcript sequence of *DNMT3a* was obtained from the *Hydractinia* genome assembly and it was fragmented into candidate probes using the pipeline available in the OligoMiner GitHub repository [16]. *Piwi1* probes were also designed. The probes were ordered from Integrated DNA Technologies and amplified using hairpin 30 and 27, with hairpin 30 used for *Piwi1* while hairpin 27 was used for *DNMT3a*. DNA cleanup was performed using the Monarch PCR and DNA cleanup kit (New England Biolabs, #T1030L) after probe concatenation. The samples were imaged using the Olympus Fluoview 3000 confocal microscope at the Centre for Microscopy and Imaging at the University of Galway. This experiment was repeated three times with multiple animals per slide and a negative control slide, where no primary probe was added.

5.4. Immunofluorescence Staining

Immunofluorescence staining was carried out as previously described in [14] but with different antibodies. For the first staining on H3K9me3, primary antibodies anti-H3K9me3 (abcam, #39065) and anti-Piwi2 (custom-made, Guinea pig.) were both diluted to 1/200. The second staining used anti-H4K16ac (ActiveMotif, Goat. #39929) and anti-Piwi2, both were diluted to 1/200. The final staining was carried out on the RFamide::GFP transgenic and it used anti-H4K16ac, anti-Piwi2 and anti-GFP (Synaptic systems, Mouse. #132005) diluted to 1/200, 1/200 and 1/400 respectively. Samples were incubated with the primary antibodies, followed by appropriate secondary antibodies including Alexa Fluor 488 (Fisher, Goat anti-rabbit. #10729174), Alexa Fluor 647 (Abcam, Goat anti-rabbit. #ab150079), Alexa Fluor 594 (Abcam, Goat anti-guinea pig. #ab150188), Alexa Fluor 488 (Abcam, Goat anti-guinea pig #ab150185) and Alexa Fluor 594 (Abcam, Goat anti-mouse. #ab150113), all diluted to 1/500. Samples were stained with 4',6-diamidino-2-phenylindole (DAPI) (1:1000 dilution of a 1mg/ml stock) before mounting and they were imaged using the Olympus Fluoview 3000 confocal microscope at the Centre for Microscopy and Imaging at the University of Galway.

5.5. Confocal Image Quantitative Analysis

Fiji was used for general image preprocessing and analysis, allowing for the visualisation, adjustment, and quantification of confocal microscopy images [17]. Brightness and contrast adjustments allowed for enhanced visualisation while reducing background noise. The Z projection tool was used to create a single 2D image from multiple optical sections of the stained nuclei. The maximum intensity projection setting kept intensity comparisons consistent across samples, reducing variability introduced by differences in Z plane focus. The confocal microscopy images are also collected in multiple channels, each corresponding to different antibody stains. Split and merge channels settings were used to isolate individual fluorophores or to visualise co-localisation between them. The region of interest (ROI) tool allowed for selection of nuclei from which statistics could be derived like mean intensity and area. The measurements used in the analysis were obtained from the base contrast and colour settings set on the confocal microscope and were not modified in any way.

5.6. Coefficient of Variation analysis using Fiji and MATLAB

The coefficient of variation (CV) is a value used to assess the compaction of DNA within the nuclei of different cell types. It measures the heterogeneity of DNA signals across the nucleus and is calculated as the ratio of the standard deviation (σ) to the mean (μ) of DAPI intensity values [18]. A protocol that was previously described was followed with modifications [18]. Fiji was used to isolate the DAPI stained image of the nuclei to be analysed and the macro script provided was ran [18]. It created masks, segmented the nuclei and generated individual nuclei for CV analysis in MATLAB. Thresholding settings in the macro script were tweaked for robust segmentation. Individual segmented nuclei were categorised by cell type into different folders and the coefficient of variation was calculated for each using a MATLAB script. P-value significant testing was also implemented into the script using Welch's t-test. This test was chosen as it does not assume equal variances between groups, which was particularly useful as the number of samples and variances were unequal. However, it is generally considered less powerful than the standard t-test.

5.7. Colocalization Testing

Colocalization testing involves measuring the overlap of pixels between two channels and calculating the Pearson's correlation coefficient (PCC) and Mander's coefficient (M1). A Fiji plugin called Just Another Colocalization Plugin (JaCoP) was utilised. The macro script from the CV analysis segmented the nuclei in the DAPI and H4K16ac channels marking them as ROIs. The plugin was then applied which overlayed these channels, enabling the assessment of their spatial relationship. Quantitative data was produced which was modelled in MATLAB.

6. Results

6.1. DNMT3a homolog identification in Hydractinia

To explore the role of DNA methylation in *Hydractinia*, we aimed to identify genes homologous to known epigenetic regulators within its genome. We identified a gene with 61% query coverage to mammalian DNMT3a after conducting a BLAST search. The gene identified (LOC130628583) had highly specific hits with key DNMT3a domains including ATRX-DNMT3-DNMT3L (ADD), DNA methyltransferase catalytic motif (DCM), and PWWP (Fig. 2C).

The *Hydractinia* single-cell atlas classifies determined cell types based on transcriptome data, and the expression matrix can identify the transcription factors and gene networks that define their identity and function (Fig. 2A). We used the atlas to spatially and transcriptionally profile DNMT3a RNA expression levels between different cell types. The expression matrix identified expression of DNMT3a across various cell types. It was notably enriched in cells associated with pluripotency and lineage specification, including i-cells, somatic cell progenitors, and gametogenesis cell types (Fig. 2B). This finding provided a foundation for further experimentation using FISH to validate the transcriptomic results.

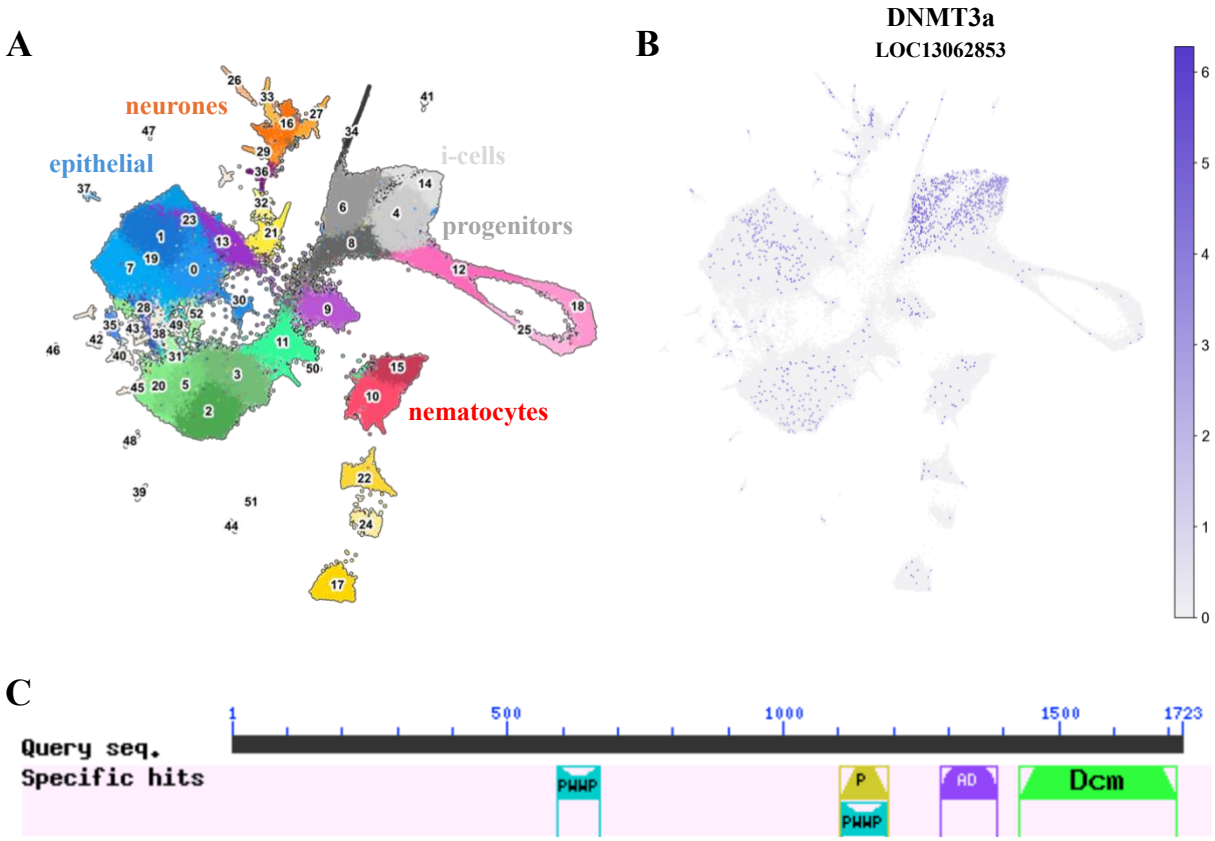

Figure 2. DNMT3a in *Hydractinia symbiolongicarpus*. ***(A)*** *UMAP projection of Hydractinia cell atlas where clusters are coloured by their cell-identity. Adapted from [14]* ***(B)*** *UMAP showing presence of LOC13062853 RNA in the dataset.* ***(C)*** *Specific domain hits identified by the CDD are shown as coloured boxes, including PWWP, AD and DCM. Numerical scale represents amino acid position. Adapted from CDD.*

6.2. SABER-FISH analysis of DNMT3a

DAPI stained labelled nuclei confirming the integrity of the samples and tissue preservation. However, no detectable signal was observed for either DNMT3a across multiple replicates. Piwi1 staining was used to display a potential overlap with DNMT3a, however it was only observed in a few i-cells, with no detectable signal in the remaining cells (Fig. 3). The same result was observed in the control experiment (Supplementary Fig. 1).

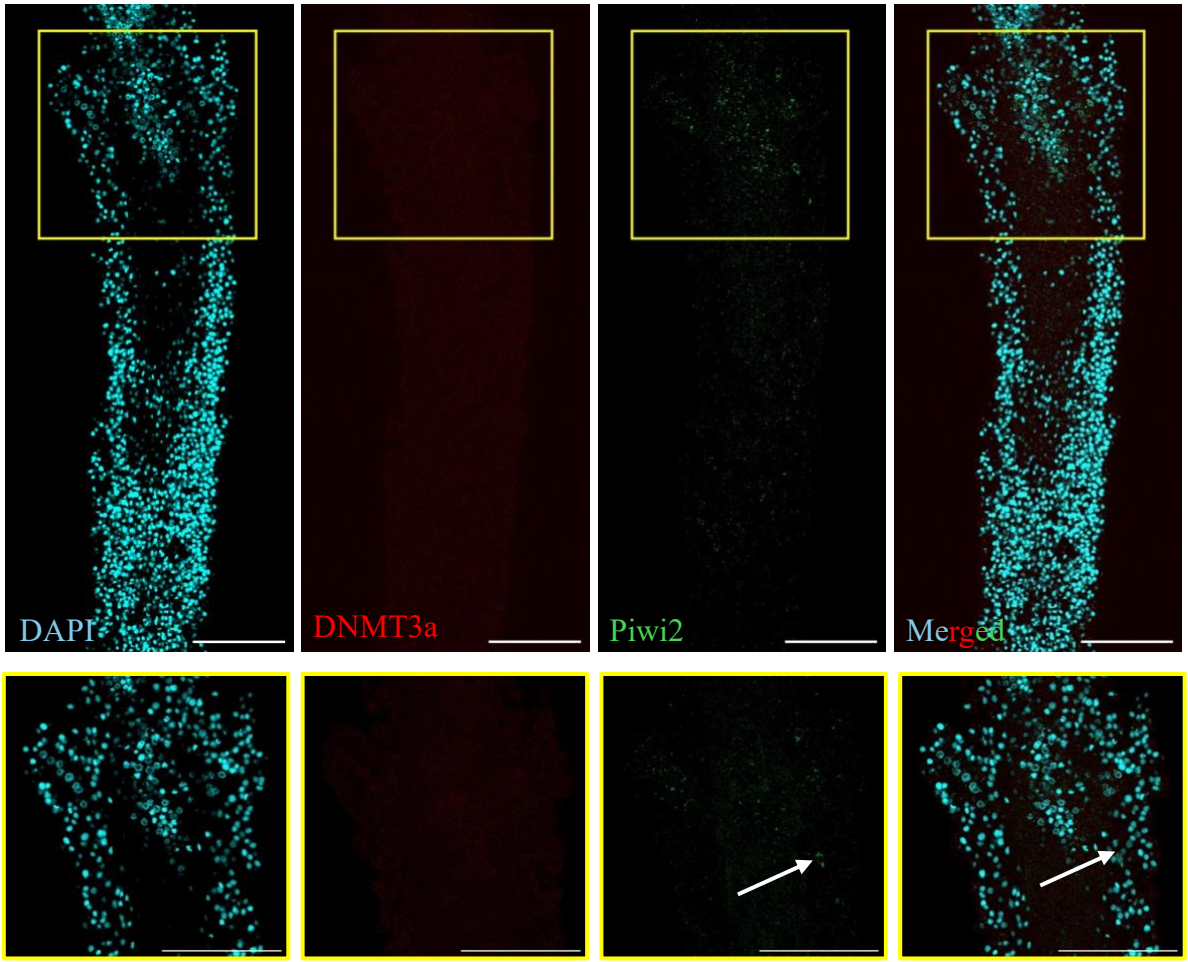

Figure 3. FISH visualisation of DNMT3a RNA localisation in i-cells. *Maximum projection of DAPI, DNMT3a and Piwi2 in a feeding polyp. White arrow points to an i-cell where successful Piwi1 staining occurred. Scale bar = 70 μm. Zoom is highlighted in yellow. The yellow boxes outline the head of the polyp.*

6.3. Histone Modifications Differ Across Distinct Cell Types

Another method to examine chromatin dynamics *in vivo* is through antibody staining of histone modifications. The first immunofluorescence staining of H3K9me3 used Piwi2, DAPI and H3K9me3. DAPI was detected in the nuclei of all cell types, revealing a distinct blue fluorescence. It was homogenously distributed reflecting typical DNA staining patterns. However, when comparing distinct cell types such as cnidocytes to i-cells, notable differences in chromatin morphology was observed. In cnidocytes the DAPI signal appeared more compact with a consistently distributed structure, likely reflecting their specialised nature. i-cells displayed large, diffuse staining with a more circular shape (Fig. 4A). Piwi2 exhibited a distinct localised pattern predominantly in the cytoplasm and sometimes in the nucleus. Piwi proteins are associated with stem cell maintenance and regulation of germline development making it invaluable for distinguishing i-cells. Piwi2 staining was primarily found at the lower part of the polyp (Fig. 4A). H3K9me3 staining successfully highlighted regions of high chromatin compaction within the nuclei. In i-cells the staining revealed distinct, concentrated foci throughout the nucleus, while the cnidocytes displayed more intense staining, particularly around the periphery. However, an issue arose during the analysis of cnidocytes, where large red ring stains likely caused by non-specific staining were observed protruding from the nuclei (Fig. 4A). This interfered with the interpretation of true H3K9me3 signals, preventing accurate quantitative analysis. A control experiment was carried out using no primary antibody to confirm the ring stains did not belong to the secondary antibody (Supplementary Fig. 2).

To circumvent this, we also decided to look at H4K16ac, a general marker for open chromatin [10]. The DAPI and Piwi2 staining pattern was the same as it was in the H3K9me3 immunofluorescence procedure. H4K16ac staining appeared in i-cells as a diffuse signal with intense speckled foci concentrated throughout the centre of the nucleus. In contrast, cnidocytes exhibited a more uniform and weak H4K16ac signal (Fig. 5A).

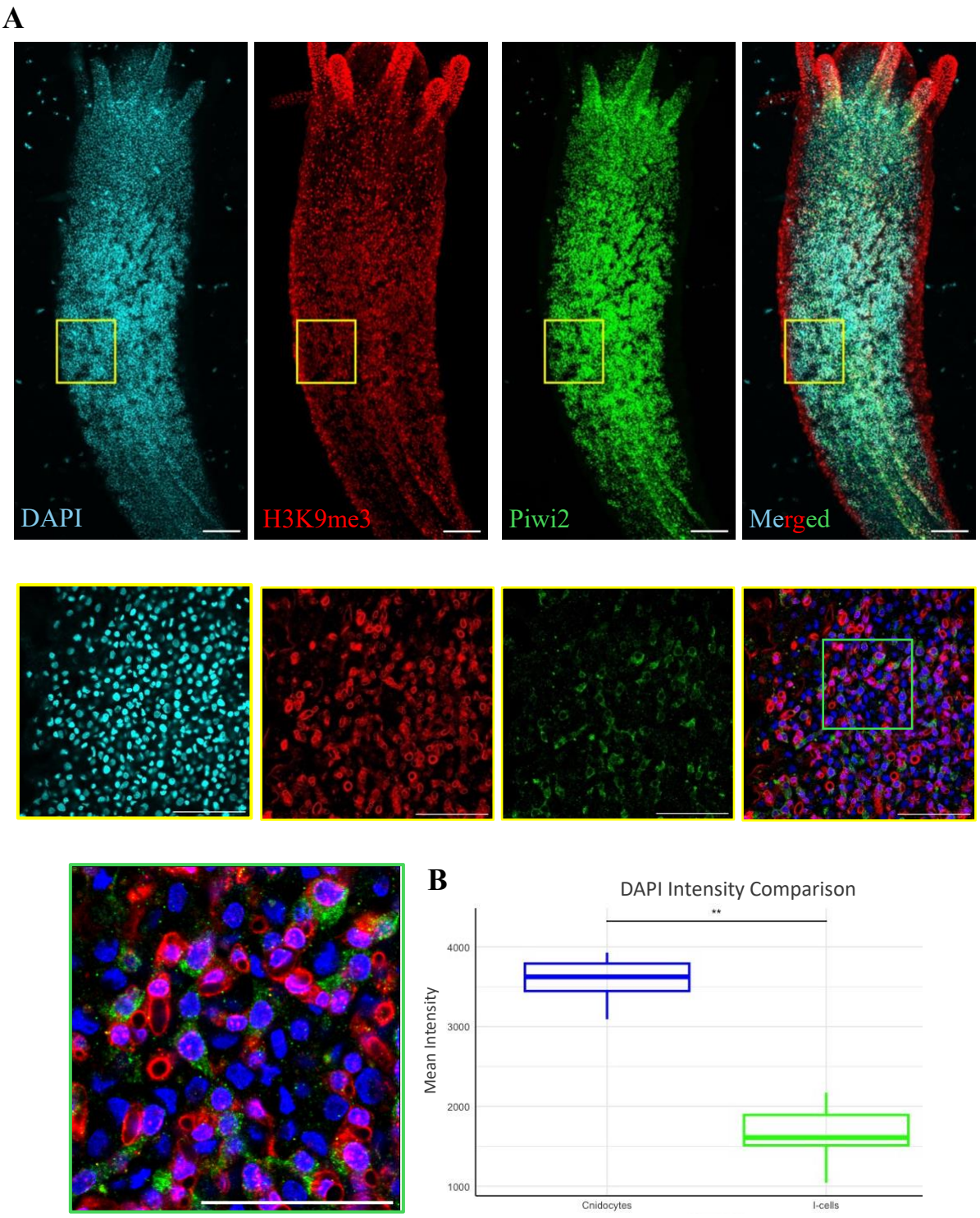

Figure 4. H3K9me3 Immunofluorescence Procedure. (A) *Maximum projection of DAPI, H3K9me3 and Piwi2 in a feeding polyp. Piwi2 exhibits strongest localisation in the central region. Scale bar = 90 µm. Zoom is highlighted in yellow. Scale bar = 20 µm. Large red rings represent non-specific H3K9me3 staining. Further zoom highlighted in green. Scale bar = 20 µm.* ***(B)*** *Mean DAPI fluorescence intensity per nucleus comparison between i-cells and cnidocytes quantified from confocal microscopy images. Welch's t-test, **p < 0.01.*

In the final immunofluorescence staining we introduced RFamide-GFP staining in addition to the H4K16ac, Piwi2 and DAPI. Rfamide is an established marker for a sub-population of neurons and the GFP which is expressed under the Rfamide promoter allowed for clear visualisation of the Rfamide+ neurons. This marker allowed for further comparison between i-cells and differentiated cells. DAPI and Piwi2 stained as they previously did in the H3K9me3 immunofluorescence procedure. i-cells appeared defined with clear borders, however there were none present in the head of the polyp (Fig. 6A). The DAPI staining in neurons showed a more compact and uneven structure. The H4K16ac did not stain effectively as the signal was weak and inconsistent across samples. There was also significant background noise. The quantitative analysis in neurons was compromised as a result.

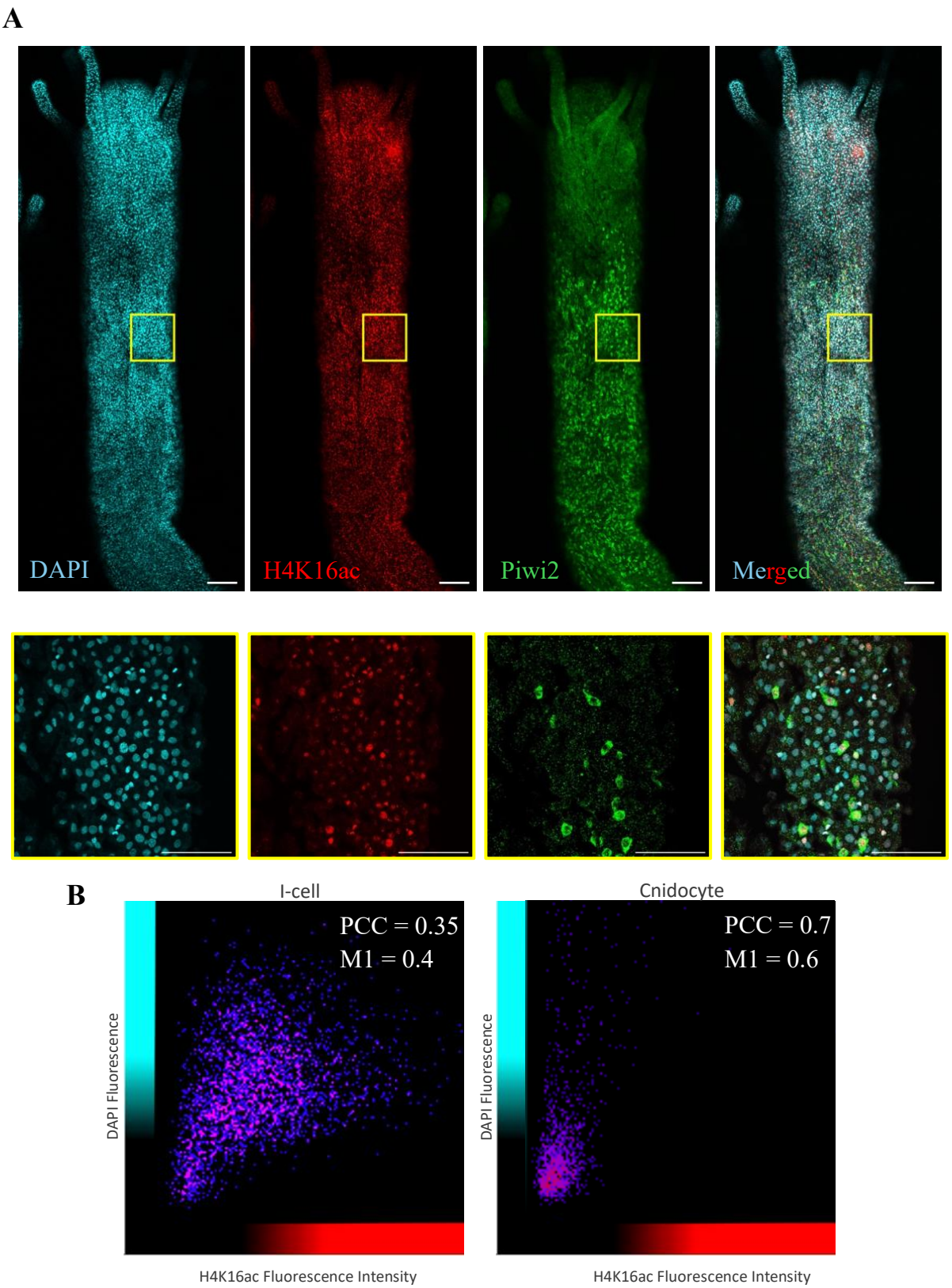

Figure 5. H4K16ac Immunofluorescence Procedure. ***(A)*** *Maximum projection of DAPI, H4K16ac and Piwi2 in a feeding polyp. Strongest H4K16ac signal aligns with Piwi2. Scale bar = 90 µm. Zoom is highlighted in yellow. Scale bar = 20 µm.* ***(B)*** *The distribution of DAPI and H4K16ac is plotted based on their fluorescence intensities in two distinct channels.*

To quantify and evaluate the observed difference in chromatin modifications and cell-specific markers we carried out statistical analysis on the intensity data. The CV was used to assess the degree of heterogeneity across the nuclei observed in i-cells, cnidocytes and neurons. i-cells exhibited the highest CV (**** $p < 0.0001$), while neurons showed an intermediate CV (** $p < 0.01$) and cnidocytes exhibited the lowest (* $p < 0.05$) (Fig. 6C). All three cell types exhibited statistically significant levels of heterogeneity reflecting the difference in their DNA packaging and accessibility. The H4K16ac analysis in neurons was interrupted because of intense background noise. However, it was possible to measure the intensity between i-cells and cnidocytes. I-cells recorded a higher mean intensity (** $p < 0.01$) than cnidocytes, indicating higher H4K16 acetylation (Fig. 4B). To further investigate H4K16ac we carried out colocalization testing between the DAPI and H4K16ac channel. The PCC assesses the correlation between intensity variations in the two channels, i-cells had a PCC of 0.35 which is considered a low colocalization but not quite independent. In cnidocytes the PCC was higher at 0.7 which is moderate. The M1 specifically measures the proportion of one signal overlapping the other. In i-cells the M1 was 0.4 and in cnidocytes it was 0.6. A fluorogram also known as an intensity scatter plot can help to visualise colocalization. There was a strong concentrated overlap between pixels in cnidocytes, while i-cells demonstrated more variance (Fig. 5B).

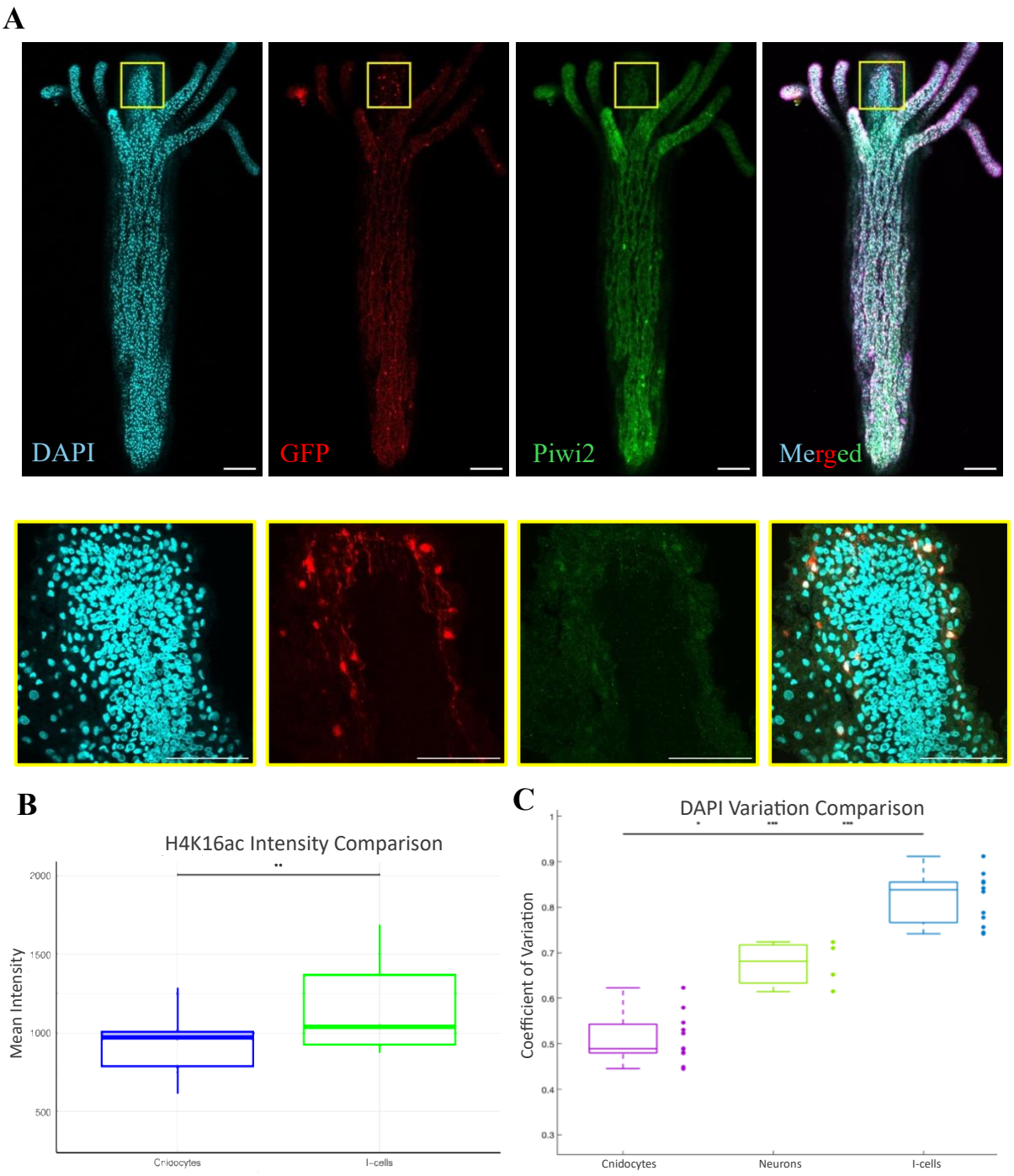

Figure 6. GFP Immunofluorescence Procedure. *Maximum projection of DAPI, GFP and Piwi2 in a feeding polyp. GFP exhibits strongest localisation in the head of the polyp. Scale bar = 90 µm. Zoom is highlighted in yellow. Scale bar = 20 µm.* ***(B)*** *Mean H4K16ac fluorescence intensity per nucleus comparison between i-cells and cnidocytes quantified from confocal microscopy images. Welch's t-test, **p < 0.01.* ***(C)*** *CV fluorescence intensity per nucleus comparison between cnidocytes, neurons and i-cells quantified from confocal microscopy images. Welch's ANOVA t-test, *p < 0.05 and ***p < 0.001.*

7. Discussion

This study aimed to further characterise the epigenetic landscape in *Hydractinia*. Using a combination of BLAST searches and single-cell transcriptomic data, we identified a DNMT3a homolog that is highly enriched in i-cells and somatic cell progenitors. While we could not confirm its presence in i-cells through FISH, the single cell data does suggest a potential role in de novo methylation during differentiation, aligning with established functions of DNMT3a in regulating cell fate [5]. Furthermore, *in vivo* immunofluorescence staining revealed distinct chromatin landscapes across different cell types. Cnidocytes and neurons exhibited highly compacted DAPI staining, characteristic of their terminally differentiated state, while i-cells displayed a more diffuse nuclear signal, indicative of higher levels of euchromatin. Histone modifications further supported these differences. H3K9me3 as a marker of heterochromatin and transcriptional repression was strongly enriched in cnidocytes. In contrast, H4K16ac is a histone modification associated with open chromatin and active transcription and it was more prominent in i-cells [10]. Conducting these experiments in an *in vivo* model ensured that the observed chromatin reflected its native biological state at fixation, which is naturally advantageous when compared with experiments done *in vitro*.

Our identification of a DNMT3a homolog in *Hydractinia* provides key insights into the conservation of DNA methylation mechanisms in cnidarians. Data reveals that the DNA methylation machinery appears highly conserved between animal phyla and was present in the metazoan common ancestor [19]. Our findings further contribute to this understanding in *Hydractinia* through the identification of conserved functional domains like ADD, PWWP, and DCM. These domains interact with histone tails and are responsible for de novo methylation, suggesting that this gene may function similarly to vertebrates [5]. DNA methylation was characterised decades ago as a repressive epigenetic marker in vertebrate regulation of cell differentiation [19]. However, vertebrates and invertebrates differ widely to the extent at which they are methylated. Invertebrate genomes are sparsely methylated while genome methylation levels in mammals are high [19]. As a result there is a consensus that DNA methylation is primarily associated with other regulatory roles in invertebrates. The enrichment of DNMT3as expression in i-cells and progenitors suggests that it may play a role in maintaining epigenetic plasticity. In mammalian systems, DNMT3a has been shown to coordinate splicing that regulates the transition from pluripotency to differentiation in embryonic and hematopoietic stem cells [19]. This raises the possibility that DNMT3a may similarly influence lineage commitment through epigenetic mechanisms in *Hydractinia*.

While our attempts to confirm DNMT3a expression in i-cells using FISH were inconclusive, several factors may have contributed to this. SABER-FISH is a complex technique where even minor deviations from the protocol can lead to weak signals or experimental failure. Proper fixation is crucial, and inadequacies can cause degradation of the sensitive RNA. DNMT3a expression could also be transient, making it difficult to detect using FISH. Strict adherence to protocol will be paramount for future attempts. While experiment repetition is a clear next step, future investigation should consider the broader DNA methylation machinery in *Hydractinia*, particularly TET enzymes and how they may influence stem cell identity and differentiation. Current research (Uri Frank Lab) is investigating sequenced methylation sites which could provide insights into how DNA methylation is regulated in response to external insults, such as radiation induced DNA damage. Further functional characterisation of DNMT3a through CRISPR knockouts and RNAi could also reveal effects on chromatin accessibility.

Immunofluorescence DAPI analysis revealed clear distinctions between different cell types based on nuclear morphology and chromatin organisation. Our cell markers, including GFP and Piwi2 effectively identified these populations. The mean and CV of DAPI intensity provided a quantitative assessment of chromatin compaction and heterogeneity. Cnidocytes and neurons exhibited high mean DAPI intensity and relatively low CVs, consistent with their compact, heterochromatic chromatin. The reduced variability aligns with their terminal differentiation, where transcription is largely fixed and the chromatin is in a stable, repressed state. i-cells displayed a lower mean intensity but a notably higher CV, reflecting their more euchromatic nature where chromatin is more open and transcriptionally active. Since euchromatin has a lower baseline staining, even small fluctuations in DAPI intensity can result in a relatively higher CV, indicating small heterochromatic regions within these progenitor cells.

Histone modifications like H3K9me3 provided further distinctions between cell types. H3K9me3 appeared to cluster around the nuclear periphery, covering a large portions of the nucleus. However, in i-cells it was observed as sparse foci scattered throughout. This peripheral enrichment may be H3K9me3-marked heterochromatin, a feature commonly associated with transcriptionally repressive domains [20]. The localisation of silent heterochromatin at the nuclear periphery may serve as a mechanism to spatially separate it from transcriptionally active euchromatin [20]. In contrast, the punctate pattern in i-cells suggests the presence of localised heterochromatic regions within an otherwise euchromatic nucleus, aligning with the high CV values observed in the DAPI analysis.

Quantification of H3K9me3 proved challenging due to the presence of non-specific staining. Cnidocytes possess a large pressurised capsule that functions in prey capture by firing harpoon-like tubules [21]. While this structure is typically identified by pronounced a-tubulin staining, it appears to have been imprecisely labelled by the H3K9me3 antibody [21]. To investigate this, a control experiment was performed with no primary antibody, resulting in no capsule staining, therefore ruling out non-specific binding of the secondary antibody. This suggests that the primary antibody may be binding to structurally similar epitopes within the capsule, potentially collagens or chitin-like proteins. This capsule staining interfered with true nuclear staining, compromising both colocalization analysis and intensity quantification. Future experiments should consider optimising blocking conditions and ordering a new batch of primary antibodies to ensure reproducibility.

H4K16ac staining revealed distinct localisation patterns between i-cells and cnidocytes. H4K16ac was observed in discrete nuclear foci in i-cells, a pattern that may reflect its role in facilitating transcriptional activation. These enrichments could correspond to genomic regions associated with active enhancers, where acetylation promotes an open chromatin state and gene expression [22]. In contrast, H4K16ac staining in cnidocytes appeared more diffuse, suggesting there are widespread chromatin modifications that do not necessarily correlate with active gene expression. This could indicate that while H4K16ac marks are present, they do not drive transcription in these terminally differentiated cells. Mander's correlation and PCC provided further insights H4K16ac and its relationship with DNA compaction. Both scores were higher in cnidocytes. Mander's indicated a greater overlap of H4K16ac with the nucleus, while PCC demonstrated that despite H4K16ac presence, DAPI intensity remained high, suggesting a more compact chromatin state. i-cells exhibited a lower Manders' correlation due to the presence of sparse, concentrated foci of H4K16ac. Additionally, the PCC suggested that regions with higher H4K16ac intensity were more likely to coincide with areas of lower DAPI intensity, consistent with a more accessible euchromatic state.

Building on the previous work on cell type-specific chromatin landscapes highlighted in this study, the findings presented here set the stage for further investigating the precise mechanisms governing stem cell pluripotency and differentiation in *Hydractinia*. The observed enrichment of a DNMT3a homolog in i-cells and progenitor populations suggests a potential role for de novo DNA methylation in developmental transitions, mirroring its function in other systems. Future research could explore this role in detail, potentially uncovering a broader function for DNMT3a in regulating epigenetic changes during cell fate commitment in *Hydractinia*. Moreover, the contrasting chromatin states are open in i-cells and more compact in differentiated cells like cnidocytes. This emphasises the importance of epigenetic modifications, such as the active H4K16ac and the repressive H3K9me3 in establishing and maintaining cellular identity. This lays the foundation for future studies aimed at understanding the interplay between these modifications and the underlying regulatory networks that define different cell types in this regenerative cnidarian model.

8. Appendices

1. hydractinia_sc_atlas GitHub repository (https://github.com/scbe-lab/hydractinia_sc_atlas)

2. OligoMiner GitHub repository (https://github.com/beliveau-lab/OligoMiner)

3. JaCoP for Colocalization tests in Fiji (https://imagej.net/plugins/jacop)

4. SABER-FISH sequences used:

Hairpins -

Hairpin 27 - ACATCATCATGGGCCTTTTGGCCCATGATGATGTATGATGATG/3InvdT/ (3' inversion to form the hairpin)

Hairpin 30 - AAATACTCTCGGGCCTTTTGGCCCGAGAGTATTTGAGAGTATT/3InvdT/ (3' inversion to form the hairpin)

Secondary probes -

For hp30 - /5Alex647N/tt GAGAGTATTT GAGAGTATTT/3InvdT/ ---- HPLC Purified

For hp27 - /5Alex565N/tt ATGATGATGT ATGATGATGT /3InvdT/ ----- HPLC Purified

Raw probes sequences -

Piwi1:

Piwi1_30.1	GGTCGTGGTGCTTCTTGACTTGGTTTACCTCTCCCCTTTAATACTCTC
Piwi1_30.2	CAGTACTTGCTTGAGGTGGTGGAGCATTTCCGCCACTTTAATACTCTC
Piwi1_30.3	TGTGTAGGCTGTGGTGCAGAACCTCTTGATCTCCCCTTTAATACTCTC
Piwi1_30.4	TGTTGTTTGGTCTGTTTGACGCAACCTCAAAATGTTAGCTTTAATACTCTC
Piwi1_30.5	ATTGGCCACAATATCAACCTTAGCGCCACCTGTGCCTTTAATACTCTC
Piwi1_30.6	ACCACAGAAGGTGAGTTTTGTGGAACCAAATTAGTGTAAGTTTTAATACTCTC
Piwi1_30.7	CCAGGCCATACTTGCATTTTGTGAGCAGGAATATCAATCTTTTTAATACTCTC
Piwi1_30.8	GCACACAACATCACATCTTGTTCATACTGCAAAATGGATGTTTTAATACTCTC
Piwi1_30.9	TTGTGAAGCTATCAGTTGGGTGTTTCTCCCAATCAATATCATTTAATACTCTC
Piwi1_30.10	GCAGCAATAAAATAGGTCCAGACATTCCTCTCTTCTTGTCCTTTAATACTCTC
Piwi1_30.11	ACACATGTGAGGATCGGCTACATTCATACCCATTGGTTTAATACTCTC

DNMT3:

DNMT3_27.1	TCATCATTAACAGATCTTGTCAGTTTAACTGGTAAATTTCATCATCAT
DNMT3_27.2	TTTACATTCAGTTGTCTAAAGGTGGTAAAGAGAAATTTCATCATCAT
DNMT3_27.3	ATCTGGATCAAAGAACAAACTCAATGTACAACAAATTTCATCATCAT
DNMT3_27.4	ATACAATTCAGAGACATCCGCATTTGATCCAGAATTTTCATCATCAT
DNMT3_27.5	TCTTACTCAGCTCTTTATCATGCACATTCCGAGTGTTTCATCATCAT
DNMT3_27.6	ACTTTATCAACCTTTGCAACTCTACCACAACCAGGTTTCATCATCAT
DNMT3_27.7	TTACTTCTCTGTCTACGTGTTGCATTCCAACAACGTTTCATCATCAT
DNMT3_27.8	CATCAATCTCAGATGCTATATAAAGTTCCACATCAAATTTCATCATCA
DNMT3_27.9	CCATCTCATCCTGAAACAGATCCTTAAGTTTCTTTTTCATCATCAT
DNMT3_27.10	TGTCATGGGAAGGCTCAGTATCAGAAGTACACTTTTCATCATCAT
DNMT3_27.11	CGCCATCACTACAAATTGTACAATACATTTGTGATTTTCATCATCAT
DNMT3_27.12	TTCTCAATGTCATAGTTTCCCTTGTGAACTCGATCTTTCATCATCAT

5. SABER-FISH control

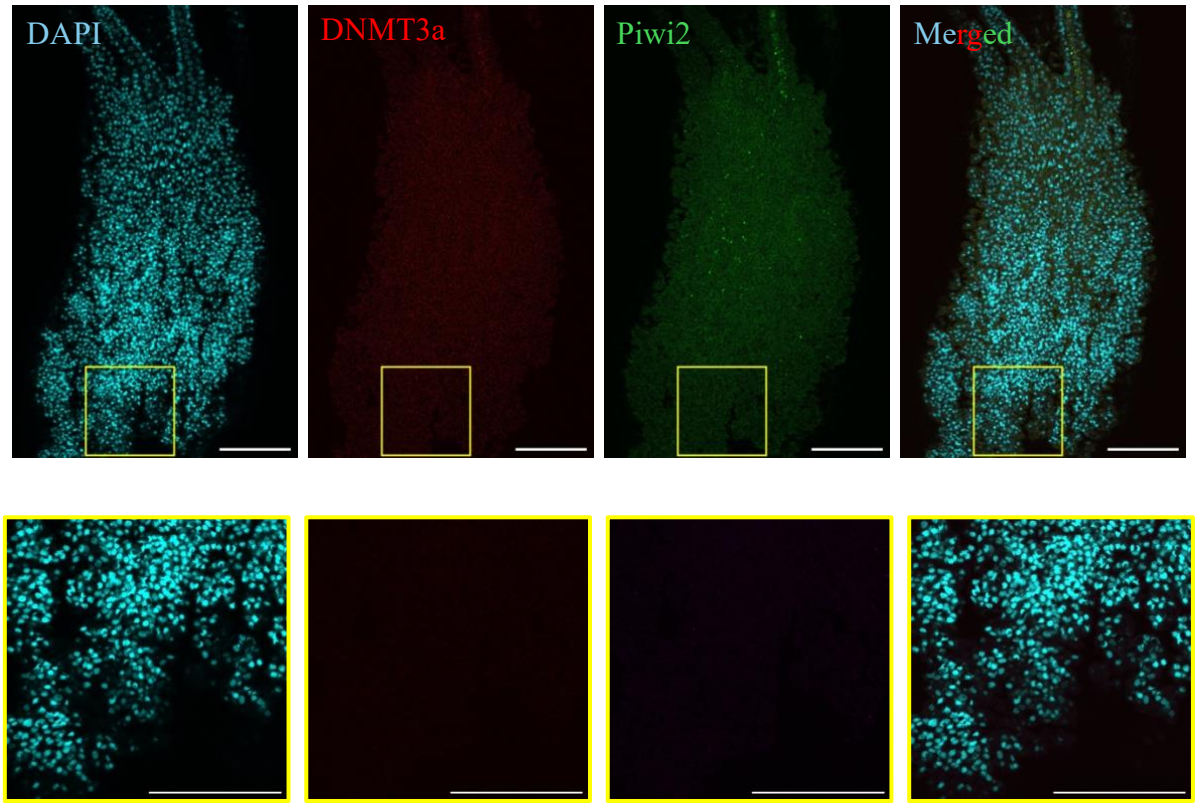

Supplementary Figure 1. FISH visualisation of DNMT3a RNA localisation in i-cells. *Maximum projection of DAPI, DNMT3a and Piwi1 in a feeding polyp. Scale bar = 70 µm. Zoom is highlighted in yellow.*

6. H3K9me3 no primary antibody control

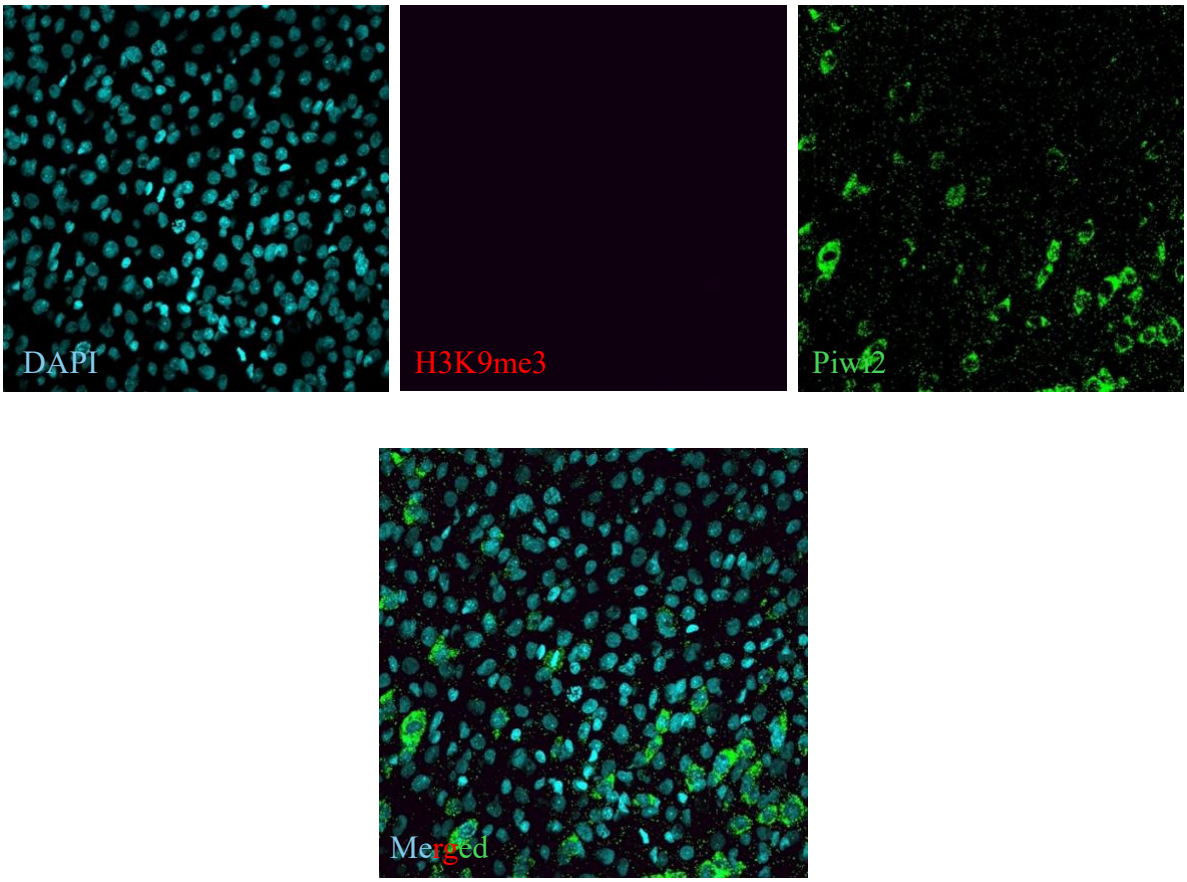

Supplementary Figure 2. H3K9me3 Immunofluorescence Procedure. (A) *Maximum projection of DAPI, H3K9me3 and Piwi2 in a feeding polyp with no primary antibody present.*

9. Bibliography

1. Kornberg RD: **Structure of chromatin**. *Annu Rev Biochem* 1977, **46**:931-954.

2. Török A, Schiffer PH, Schnitzler CE, Ford K, Mullikin JC, Baxevanis AD, Bacic A, Frank U, Gornik SG: **The cnidarian Hydractinia echinata employs canonical and highly adapted histones to pack its DNA**. *Epigenetics Chromatin* 2016, **9**:36.

3. Morrison O, Thakur J: **Molecular Complexes at Euchromatin, Heterochromatin and Centromeric Chromatin**. *Int J Mol Sci* 2021, **22**:28.

4. Pillai A, Gungi A, Reddy PC, Galande S: **Epigenetic Regulation in Hydra: Conserved and Divergent Roles**. *Front Cell Dev Biol* 2021, **9**:663208.

5. Chen Z, Zhang Y: **Role of Mammalian DNA Methyltransferases in Development**. *Annu Rev Biochem* 2020, **89**:135-158.

6. Pillai A, Gungi A, Reddy PC, Galande S: **Epigenetic Regulation in Hydra: Conserved and Divergent Roles**. *Front Cell Dev Biol* 2021, **9**:663208.

7. Paksa A, Rajagopal J: **The epigenetic basis of cellular plasticity**. *Curr Opin Cell Biol* 2017, **49**:116-122.

8. Dimitrova E, Turberfield AH, Klose RJ: **Histone demethylases in chromatin biology and beyond**. *EMBO Rep* 2015, **16**:1620-1639.

9. Dormann HL, Tseng BS, Allis CD, Funabiki H, Fischle W: **Dynamic regulation of effector protein binding to histone modifications: the biology of HP1 switching**. *Cell Cycle* 2006, **5**:2842-2851.

10. Dou Y, Milne TA, Tackett AJ, Smith ER, Fukuda A, Wysocka J, Allis CD, Chait BT, Hess JL, Roeder RG: **Physical association and coordinate function of the H3 K4 methyltransferase MLL1 and the H4 K16 acetyltransferase MOF**. *Cell* 2005, **121**:873-885.

11. Weismann A: ***Das Keimplasma: eine Theorie der Vererbung***. Jena: Gustav Fischer; 1892.

12. Chrysostomou E, Flici H, Gornik SG, Salinas-Saavedra M, Gahan JM, McMahon ET, Thompson K, Hanley S, Kilcoyne M, Schnitzler CE, et al.: **A cellular and molecular analysis of SoxB-driven neurogenesis in a cnidarian**. *Elife* 2022, **11**:24.

13. Plickert G, Frank U, Müller WA: **Hydractinia, a pioneering model for stem cell biology and reprogramming somatic cells to pluripotency**. *Int J Dev Biol* 2012, **56**:519-534.

14. Salamanca-Diaz DA, Horkan HR, Garcia-Castro H, Emili E, Salinas-Saavedra M, Perez-Posada A, Rossi ME, Alvarez-Presas M, Mac Gabhann R, Hillenbrand P, et al.: **The Hydractinia cell atlas reveals cellular and molecular principles of cnidarian coloniality**. *Nat Commun* 2025, **16**:2121.

15. Frank U, Nicotra ML, Schnitzler CE: **The colonial cnidarian Hydractinia**. *Evodevo* 2020, **11**:7.

16. Kon-Nanjo K, Kon T, Horkan HR, Febrimarsa, Steele RE, Cartwright P, Frank U, Simakov O: **Chromosome-level genome assembly of Hydractinia symbiolongicarpus**. *G3 (Bethesda)* 2023, **13**:9.

17. Schindelin J, Arganda-Carreras I, Frise E, Kaynig V, Longair M, Pietzsch T, Preibisch S, Rueden C, Saalfeld S, Schmid B, et al.: **Fiji: an open-source platform for biological-image analysis**. *Nat Methods* 2012, **9**:676-682.

18. Martin L, Vicario C, Castells-Garcia A, Lakadamyali M, Neguembor MV, Cosma MP: **A protocol to quantify chromatin compaction with confocal and super-resolution microscopy in cultured cells**. *STAR Protoc* 2021, **2**:100865.

19. Ying H, Hayward DC, Klimovich A, Bosch TCG, Baldassarre L, Neeman T, Foret S, Huttley G, Reitzel AM, Fraune S, et al.: **The Role of DNA Methylation in Genome Defense in Cnidaria and Other Invertebrates**. *Mol Biol Evol* 2022, **39**:14.

20. Kiseleva AA, Cheng YC, Smith CL, Katz RA, Poleshko A: **PRR14 organizes H3K9me3-modified heterochromatin at the nuclear lamina**. *Nucleus* 2023, **14**:2165602.

21. Plachetzki DC, Fong CR, Oakley TH: **Cnidocyte discharge is regulated by light and opsin-mediated phototransduction**. *BMC Biol* 2012, **10**:17.

22. Pal D, Patel M, Boulet F, Sundarraj J, Grant OA, Branco MR, Basu S, Santos SDM, Zabet NR, Scaffidi P, et al.: **H4K16ac activates the transcription of transposable elements and contributes to their cis-regulatory function**. *Nat Struct Mol Biol* 2023, **30**:935-947.